Attosecond Spectral Shearing Interferometry

F. Quéré,* J. Itatani, G. L. Yudin, and P. B. Corkum

Steacie Institute for Molecular Sciences, National Research Council of Canada, Ottawa, Ontario, Canada K1A 0R6

(Received 18 December 2001; published 21 February 2003)

We show that the complete characterization of arbitrarily short isolated attosecond x-ray pulses can be achieved by applying spectral shearing interferometry to photoelectron wave packets. These wave packets are coherently produced through the photoionization of atoms by two time-delayed replicas of the x-ray pulse, and are shifted in energy with respect to each other by simultaneously applying a strong laser field. The x-ray pulse is reconstructed with the algorithm developed for optical pulses, which requires no knowledge of ionization physics. Using a 800-nm shearing field, x-ray pulses shorter than ~400 asec can be fully characterized.

DOI: 10.1103/PhysRevLett.90.073902 PACS numbers: 42.65.Ky, 32.80.Wr, 41.50.+h, 42.65.Re

The production of single attosecond (1 asec = 1×10^{-18} sec) soft-x-ray pulses [1,2] has opened the route to probing electronic dynamics in atoms, molecules, and solids [3]. However, accurately characterizing their temporal profile is a challenge that must be overcome if attosecond science is to develop rapidly. Several methods have been proposed to determine the pulse duration [2,4,5], mostly based on the photoionization of atoms by the x-ray pulse in the presence of a strong laser field. The best resolution estimated thus far is ~100 asec [5]. None of these methods, however, completely characterizes the attosecond pulse, because they do not fully measure its phase properties.

One method for the complete characterization of ultrashort visible light pulses is spectral phase interferometry for direct electric-field reconstruction (SPIDER) [6]. SPIDER measures the relative phases of the different frequency components. Critical to SPIDER is a frequency shift $\Delta\Omega$ induced between two replicas of the light pulse to be characterized, delayed by a time τ. If $\tilde{E}(\Omega) = A(\Omega)e^{i\varphi(\Omega)}$ is the spectrum of the unknown pulse, then the total spectral intensity $S_T(\Omega)$ of these frequency-shifted twin pulses is given by

$$S_T(\Omega) = |\tilde{E}(\Omega) + e^{i\Omega\tau}\tilde{E}(\Omega - \Delta\Omega)|^2. \quad (1)$$

The two pulses interfere in the frequency domain and, because of the time shift τ, $S_T(\Omega)$ has fringes. The frequency shift $\Delta\Omega$ causes a modulation to the positions of these fringes, which provides information on the slowly varying spectral phase $\varphi(\Omega)$.

$\varphi(\Omega)$ can be retrieved from three experimentally measured quantities, $S_T(\Omega)$, τ, and $\Delta\Omega$ [6]. Knowing $A(\Omega)$—which is measured independently with a spectrometer—and $\varphi(\Omega)$, the full temporal profile of the pulse is obtained by a Fourier transformation.

SPIDER cannot be directly applied to attosecond x-ray pulses, because no nonlinear optical process is available in this spectral range to induce the frequency shift $\Delta\Omega$. We demonstrate that the spectral phase of these pulses can be measured by applying SPIDER to photoelectron wave packets. These wave packets are produced by the photoionization of atoms, in the presence of a laser field, by two delayed but otherwise identical replicas of the attosecond x-ray pulse. The laser field provides the energy (frequency) shift between these wave packets. We thus determine the phase structure of the wave packet, from which the spectral phase of the attosecond x-ray pulse can be directly deduced.

We first describe attosecond SPIDER qualitatively, then, using the strong field approximation, we derive equations that prove the connection with optical SPIDER. Finally, we simulate an experiment and apply the usual SPIDER reconstruction algorithm to retrieve the pulse that we assumed in the simulation.

Qualitatively, two replicas of the x-ray pulse, shifted in time by τ, have a modulated optical spectrum S_T, and therefore generate a modulated photoelectron spectrum S_e. An alternative interpretation of these fringes is that the two x-ray pulses generate two identical wave packets, shifted in time, which interfere just as light pulses, and thus produce the fringes in S_e: The measurement of S_e is spectral interferometry with wave packets [7].

The energy shift between these two wave packets can be induced by ionizing the atoms in the presence of a time-dependent electric field. We will assume that the field consists of an intense linearly polarized laser field $\mathbf{E}_L(t') = E_0(t')\cos(\omega_L t')\mathbf{e}_L$. In this case, the final energy W of an electron ionized at time t by the absorption of one x-ray photon is, according to classical mechanics [2,5],

$$W \approx W_0 + 2U_p \cos 2\theta \sin^2\omega_L t + \sqrt{8W_0U_p}\cos\theta \sin\omega_L t, \quad (2)$$

where W_0 is the electron energy at the time of ionization, $U_p = E_0^2/4\omega_L^2$ ($\ll W_0$) is the ponderomotive energy (atomic units are used throughout the paper), and θ is the angle of observation of the photoelectron, measured from the polarization direction $\mathbf{e}_L$ of the laser field.

The laser field induces a change $\delta W = W - W_0$ of the electron energy. δW depends on the peak strength

$E_0(t)$ and the phase $\omega_L t$ of the laser field at the time of ionization, and on the observation angle θ. If the x-ray field consists of two identical pulses, centered at $t = t_0$ and $t = t_0 + \tau$, and short compared to the laser period, the laser field induces a well-defined energy shift $\Delta W = \delta W(t_0 + \tau) - \delta W(t_0)$ between the two corresponding wave packets, provided that we observe the photoelectrons in a given direction, and choose the phase of the laser field and the delay between the x-ray pulses appropriately.

Of the possible angles of observation, Eq. (2) shows that, at $\theta = \pi/2$, the energy shift ΔW is independent of the photoelectron energy just as it is in optical SPIDER. At $\theta = \pi/2$, of the possible delays between the twin pulses, the maximum energy shift $2U_p$ occurs when they are separated by $\omega_L \tau = 2\pi(n/2 + 1/4)$ and phased so one is synchronized to the peak of the electric field ($\omega_L t_0 = 0$) and the other to the zero crossing.

We now confirm this qualitative discussion, using the strong field approximation [8,9] to derive an equation for attosecond SPIDER that is analogous to Eq. (1). The transition amplitude to the final continuum state $|\mathbf{v}\rangle$ with momentum $\mathbf{v}$ is given by

$$a_{\mathbf{v}} = -i \int_{-\infty}^{+\infty} dt\, \mathbf{d}_{\mathbf{p}(t)} \mathbf{E}_X(t) e^{-i \int_t^{+\infty} dt' [\mathbf{p}^2(t')/2 + I_p]}, \qquad (3)$$

$\mathbf{E}_X(t)$ is the x-ray electric field. $\mathbf{p}(t) = \mathbf{v} + \mathbf{A}(t)$ is the instantaneous momentum of the free electron in the laser field, $\mathbf{A}(t)$ being the vector potential of this field, such that $\mathbf{E}_L(t) = -\partial \mathbf{A}/\partial t$. $\mathbf{d}_{\mathbf{p}(t)}$ is the dipole transition matrix element from the ground state to the continuum state with momentum $\mathbf{p}(t)$. I_p is the ionization potential of the atom. We define $\Phi(t, \mathbf{v})$ as the integral in the exponential of Eq. (3). $\Phi(t, \mathbf{v}) - I_p t$ is the phase acquired by an electron with an initial momentum $\mathbf{p}(t)$ at the time of ionization t, during its motion in the continuum from t to $+\infty$, in the presence of the laser field.

When the x-ray field consists of twin pulses, and these pulses are much shorter than the laser period, the photoelectron energy spectrum $S_e(W) = |a_{\mathbf{v}}|^2$ is given by

$$S_e(W) = |\mathbf{d}_{\mathbf{p}(t_0)} \mathbf{F}_{t_0}(W) + e^{i[W\tau + \chi]} \mathbf{d}_{\mathbf{p}(t_0+\tau)} \mathbf{F}_{t_0+\tau}(W)|^2,$$

$$\mathbf{F}_{t_X}(W) = \int_{-\infty}^{+\infty} dt\, \mathbf{E}_X(t) e^{i[W - \delta W(W_0, t_X) + I_p](t - t_X)}, \qquad (4)$$

$$\chi = [U_p + I_p]\tau + \Delta\Phi_1 + \Delta\Phi_2,$$

with $t_X = t_0$ or $t_0 + \tau$, $\Delta\Phi_1 = -(U_p/2\omega_L)[\sin 2\omega_L t]_{t_0}^{t_0+\tau}$, and $\Delta\Phi_2 = (\sqrt{8U_p W}/\omega_L)\cos\theta [\cos\omega_L t]_{t_0}^{t_0+\tau}$. As long as $U_p \ll W_0/2$, $\delta W(W_0, t)$ in Eq. (4) can be deduced from Eq. (2) [5].

Equation (4) is almost identical to Eq. (1) that describes optical SPIDER. An energy shift $\Delta W = \delta W(t_0 + \tau) - \delta W(t_0)$ arises from the integral for $\mathbf{F}_{t_X}(W)$ evaluated at $t_X = t_0$ and $t_X = t_0 + \tau$. ΔW corresponds to the spectral shift $\Delta\Omega$ in Eq. (1). The term $W\tau$ corresponds to $\Omega\tau$ in Eq. (1), and is responsible for the appearance of fringes. Equation (4) thus describes interference of spectrally sheared photoelectron wave packets generated by twin attosecond pulses. This SPIDER spectrum therefore gives access to the spectral phase of $d_{\mathbf{p}} \tilde{E}_X(\Omega)$ [where $\tilde{E}_X(\Omega)$ is the spectrum of the x-ray field], i.e., to the spectral phase of the electron wave packet.

There are two effects in Eq. (4) that do not occur in the optical analogue: In general, χ and ΔW depend on the photoelectron energy W. However, at $\theta = \pi/2$, both dependences vanish and Eq. (4) exactly maps onto optical SPIDER [Eq. (1)]. At other angles, χ is constant only if we choose the delay τ between the x-ray pulses and the phase of the laser field so that $[\cos\omega_L t]_{t_0}^{t_0+\tau} = 0$ (i.e., $\Delta\Phi_2 = 0$), and the energy dependence of ΔW can be neglected if the spectral width $\Delta\Omega_X$ of the x-ray pulse is small enough [i.e., $\partial(\Delta W)/\partial W_0 \cdot \Delta\Omega_X \ll \Delta W$]. With the energy dependences of χ and ΔW minimized, the conventional SPIDER algorithm [6] can be used directly.

To retrieve the spectral phase of the x-ray pulse, the frequency dependence of the phase of the dipole transition matrix element $\mathbf{d}_{\mathbf{p}}$ must be known. The dipole phase can be obtained analytically in the case of a one-electron atom. For a two-electron atom (e.g., He), the dipole phase can be calculated if the x-ray photon energy is above the two-electron ionization threshold. The energy dependence of $|\mathbf{d}_{\mathbf{p}}|$ does not affect the spectral phase obtained by this method, just as the spectral dependence of the upconversion efficiency does not affect optical SPIDER [6].

We now use Eq. (3) to simulate an experiment. In the simulations, $\mathbf{d}_{\mathbf{p}}$ is assumed to be constant for simplicity. Figure 1(a) shows two photoelectron spectra observed in the perpendicular direction ($\theta = \pi/2$), generated by a transform-limited Gaussian x-ray pulse of duration $\tau_X = 12.5$ asec (≈ 0.5 a.u., FWHM of intensity profile), in the presence of a laser field. Although such an x-ray pulse duration is beyond what can presently be achieved experimentally [2], we choose these parameters to demonstrate that there is no minimum time resolution limit that is intrinsic to SPIDER.

The full line in Fig. 1(a) corresponds to $\omega_L t_0 = 0$ (the first pulse at the peak of the laser electric-field), and the dotted one to $\omega_L(t_0 + \tau) = \pi/2$ (the second pulse at the zero crossing of the laser electric-field). As expected from Eq. (2), the first of these spectra is identical to the one obtained in the absence of the laser field (dots), while the second one is an undistorted copy shifted by $-2U_p$. These spectra do not change even if the x-ray pulse is chirped, as long as other parameters are kept constant.

Figure 1(b) shows the photoelectron spectrum when both pulses ionize the atom in the presence of the laser field. Interference fringes of periodicity $\sim 4\omega_L$ are observed because of the time separation $\tau = \pi/2\omega_L$ between the pulses. The detailed structure of these fringes depends on the spectral phase of the x-ray pulse. This is

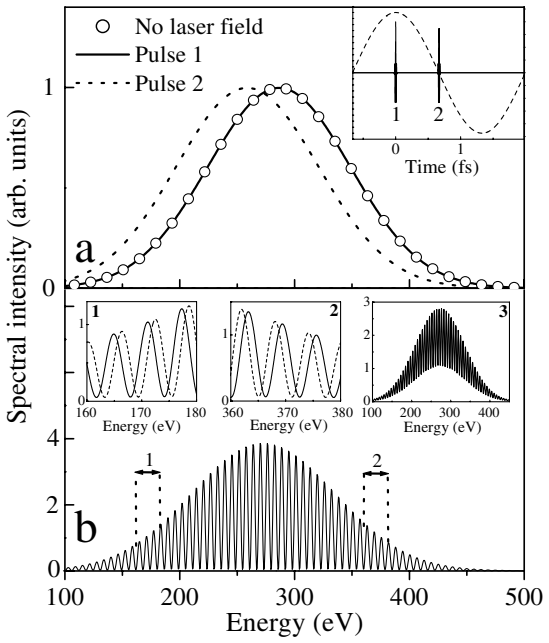

FIG. 1. (a) Photoelectron spectra from hydrogen atoms ($I_p = 13.6$ eV) at $\theta = \pi/2$, produced by each of the two x-ray pulses shown in the inset ($\tau_X = 12.5$ asec, $\xi = 0$, $\Omega_X = 300$ eV) in the presence of a laser field ($\lambda = 800$ nm, $I = 230\ \mathrm{TW/cm^2}$, $U_p = 13.8$ eV). The open circles show the spectrum obtained in the absence of the laser field. The dashed line in the inset shows the laser field. (b) Photoelectron spectrum obtained when both pulses successively excite the atom in the laser field. Insets 1 and 2 compare the interference patterns obtained with $\xi = 0$ (full line) and $\xi = 4$ (dashed line). Inset 3 shows the spectrum obtained when $\omega_L t_0$ fluctuates, following a Gaussian distribution with a 10° FWHM.

illustrated in insets 1 and 2 of Fig. 1(b), where we compare the fringes obtained for transform-limited ($\tau_X = 12.5$ asec) and linearly chirped ($\tau_X = 50$ asec, $\xi = 4$) pulses with the same spectral width $\Delta\Omega_X$. Here ξ is a dimensionless chirp parameter [5], and $\tau_X \sim \sqrt{1 + \xi^2}/\Delta\Omega_X$. In these conditions, when the pulse is positively chirped, the fringes are observed to shift to higher energies on the low-energy side of the spectrum, and to lower energies on the high-energy side. The reverse would occur for a negatively chirped pulse. At the center of the spectrum, the fringes are unaffected by the chirp. In other words, information on the spectral phase is provided by the fringe spacing.

To reconstruct $\varphi(W)$ from the photoelectron spectrum, we use the same algorithm as in conventional SPIDER [6]. It consists of the following steps. (i) The SPIDER spectrum is Fourier transformed, (ii) a spectral window is applied to the positive-frequency branch of this function, (iii) this filtered function is inversely Fourier transformed to obtain $\Delta\varphi(W) = \varphi(W - \Delta W) - \varphi(W)$, and then (iv) $\Delta\varphi(W)$ is integrated to get the spectral phase $\varphi(W)$. The circles in Fig. 2 show the spectral phase $\varphi(W)$ obtained when the algorithm is applied to the simulated spectrum shown in Fig. 1 corresponding to the chirped pulse. As can be seen, it reproduces the x-ray spectral phase $\varphi(W)$ (full line) very accurately.

The squares in Fig. 2 show the spectral phase $\varphi(W)$ deduced from an interferometric photoelectron spectrum S_e measured in the direction $\theta = 0$, using the conventional SPIDER retrieval algorithm. We use the same x-ray pulse as in Fig. 1 ($\xi = 4$, $\tau_X = 50$ asec). The laser intensity is now $1.4\ \mathrm{TW/cm^2}$, with $\omega_L t_0 = -\pi/2$ and $\omega_L(t_0 + \tau) = \pi/2$—leading to the maximum energy shift $\sqrt{8W_0U_p}$ between the two wave packets. At $\theta = 0$, the energy shear ΔW depends on the photoelectron energy, and the conventional SPIDER algorithm is no longer exact, as can be seen from the slight difference between the retrieved and exact spectral phases in Fig. 2.

Figure 2 confirms that, for measurements at $\theta = \pi/2$, we can apply the phase retrieval algorithm developed for optical pulses [6] without modification. No knowledge of ionization physics is needed. In other directions, the SPIDER spectra can still be measured but, for accurate phase reconstruction, a small modification is needed in the last step (iv) of the retrieval algorithm to take into account the dependence of the laser-induced energy shift on the x-ray photon energy.

The angle dependence of SPIDER results implies that the finite acceptance angle of an electron spectrometer affects the measurement. Both ΔW and $\Delta\Phi_2$ in Eq. (4) depend on the observation angle θ, so that increasing the collection angle of the photoelectrons leads to a reduction of the fringe contrast. At $\theta = 0$, the angular dependence does not impose a severe limitation because $\partial(\Delta W)/\partial\theta = \partial(\Delta\Phi_2)/\partial\theta = 0$. Our calculations show that an angular acceptance as large as 40° is adequate for the conditions considered above. This large angular acceptance is a major advantage of this configuration. At $\theta = \pi/2$, both derivatives are nonzero, so that the angular acceptance is reduced to ~2°.

We see no impediment to attosecond SPIDER experiments. In high-harmonic generation, the most likely

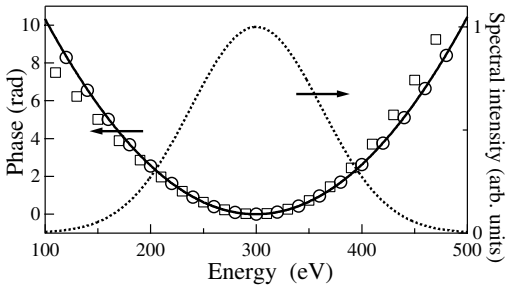

FIG. 2. Comparison between the spectral phases retrieved from SPIDER spectra and the exact spectral phase $\varphi(W)$ ($\xi = 4$, full line). Circles: retrieved from the spectrum in Fig. 1(b) ($\theta = \pi/2$). Squares: retrieved from the spectrum measured at $\theta = 0$. In both cases, the energy shift $\Delta W \approx 27$ eV. The dotted line shows $|\tilde{E}_X(\Omega)|^2$.

source of attosecond pulses, the x-ray pulses are phase locked and collinear to the driving laser pulse, which therefore provides an ideal dressing field to induce the energy shift. The fringe spacing is of the order of several eV, which is easily resolved with an electron spectrometer. Retrieving the spectral phase from the SPIDER spectrum requires knowledge of the delay τ and the energy shift ΔW. τ is deduced from the fringe spacing in the absence of the laser field, while ΔW is measured by alternatively blocking each of the twin x-ray pulses. Two replicas of a single attosecond x-ray pulse can be produced using a comblike mirror, with a teeth depth of $\sim$ 100 nm. Each pulse reflects from a different depth, and we use the zero order signal from this "grating." If this mirror is made out of one block of material, shot-to-shot fluctuations in the delay τ are avoided.

Adjusting the relative phase $\omega_L t_0$ of the laser field with respect to the x-ray pulses requires some moving parts, which could introduce shot-to-shot fluctuations in this phase. Their effect on the energy shift ΔW will be minimized, since we chose t_0 to satisfy $\partial(\Delta W)/\partial t\,|_{t=t_0} = 0$. However, changes in t_0 affect the phase shift χ induced between the two wave packets by the laser field. Therefore, the fluctuations in t_0 will result in a blur of the fringes, and reduce their contrast, as seen in inset 3 of Fig. 1(b). Provided that the fringes are visible, this does not induce any error in the phase retrieval. For a given fluctuation amplitude, the blurring of the fringes increases with the laser intensity. This will limit the maximum energy shift that can be induced, and, consequently, the ultimate temporal resolution of attosecond SPIDER.

Individual femtosecond x-ray pulses [10], as well as trains of attosecond pulses as short as 250 asec [11], have been characterized using the sidebands induced in the photoelectron spectrum by the laser field. Before concluding, we present an analysis which connects these methods to the attosecond streak camera [5] and attosecond SPIDER.

Assuming that the laser field varies as $\mathbf{E}_L(t) = \mathbf{E}_0 \cos(\omega_L t)$, the transition amplitude $a_{\mathbf{v}}$ can be calculated analytically for any x-ray field:

$$a_{\mathbf{v}} = \sum_{m,n=-\infty}^{+\infty} (-1)^m i^n J_m(M) J_n(N) \tilde{R}_X(W + I_p + \omega_{mn}), \quad (5)$$

where W is the final energy of the photoelectron, $J_k(z)$ are the Bessel functions, $M = U_p/2\omega_L$, $N = 2\sqrt{U_p}(\mathbf{v}\cdot\mathbf{e}_L)/\omega_L$, $\omega_{mn} = \omega_L(2M + 2m + n)$, and $\tilde{R}_X(\omega)$ is the Fourier transform of $R_X(t) = \mathbf{d}_{\mathbf{p}(t)}\mathbf{E}_X(t)$. Equation (5) shows that the photoelectron spectrum consists of an ensemble of sidebands. These sidebands are induced by the $\mathbf{A}^2(t)$ and the $\mathbf{v}\cdot\mathbf{A}(t)$ terms in $\Phi(t, \mathbf{v})$ [see Eq. (3)], which, respectively, lead to the $J_m(M)$ and $J_n(N)$ terms in Eq. (5). The first kind of sidebands extends up to $|m| \sim M$ with a spacing of $2\omega_L$, while the second kind extends up to $|n| \sim N$ with a spacing of ω_L. There is also a correspondence between these two processes and the second and third terms on the right-hand side of Eq. (2), derived using classical mechanics.

In the case of a single x-ray pulse shorter than the laser period, the sidebands broaden and overlap. The photoelectron spectrum therefore depends on their interferences. By appropriately choosing the laser phase, these interferences can either lead to spectral distortions that are used in the attosecond streak camera [5], or can shift the whole photoelectron spectrum without distortion, making attosecond SPIDER possible.

In conclusion, we introduced a method for measuring extremely short ($\sim$ 1 a.u.) x-ray pulses. However, attosecond SPIDER also allows measurement of currently accessible pulses. For example, using parallel observation, an 800-nm 10-GW/cm^2 shearing field, and with the twin pulses separated by 1.5 periods, we can reconstruct the spectral phase of a 400-asec pulse centered at 100 eV. 400-asec pulses are near the upper limit for accurate reconstruction using 800-nm shearing fields.

Discussions with M. Yu. Ivanov, I. A. Walmsley, T. Seideman, and H. G. Muller are gratefully acknowledged. This work was partly supported by Photonics Research Ontario.

*Current address: CEA/DSM/DRECAM/SPAM, CEA Saclay, 91 191 Gif-sur-Yvette, France.

[1] T. Brabec and F. Krausz, Rev. Mod. Phys. **72**, 545 (2000), and references therein.
[2] M. Drescher *et al.*, Science **291**, 1923 (2001); M. Hentschel *et al.*, Nature (London) **414**, 509 (2001).
[3] M. Drescher *et al.*, Nature (London) **419**, 803 (2002).
[4] E. Constant *et al.*, Phys. Rev. A **56**, 3870 (1997); Y. Kobayashi *et al.*, Opt. Lett. **23**, 64 (1998); A. Scrinzi, M. Geissler, and T. Brabec, Phys. Rev. Lett. **86**, 412 (2001).
[5] J. Itatani *et al.*, Phys. Rev. Lett. **88**, 173903 (2002); M. Kitzler *et al.*, Phys. Rev. Lett. **88**, 173904 (2002).
[6] C. Iaconis and I. A. Walmsley, Opt. Lett. **23**, 792 (1998); IEEE J. Quantum Electron. **35**, 501 (1999).
[7] T. C. Weinacht, J. Ahn, and P. H. Bucksbaum, Phys. Rev. Lett. **80**, 5508 (1998).
[8] A. M. Dykhne and G. L. Yudin, Usp. Fiz. Nauk **121**, 157 (1977) [Sov. Phys. Usp. **20**, 80 (1977)]; **125**, 377 (1978) [*ibid.* **21**, 549 (1978)].
[9] M. Lewenstein *et al.*, Phys. Rev. A **49**, 2117 (1994).
[10] J. M. Schins *et al.*, Phys. Rev. Lett. **73**, 2180 (1994); T. E. Glover *et al.*, Phys. Rev. Lett. **76**, 2468 (1996); A. Bouhal *et al.*, J. Opt. Soc. Am. B **14**, 950 (1997); E. S. Toma *et al.*, Phys. Rev. A **62**, 061801(R) (2000).
[11] P. M. Paul *et al.*, Science **292**, 1689 (2001); H. G. Muller, Appl. Phys. B **74**, S17 (2002).